WRC RESEARCH REPORT NO. 16

NON-DARCY FLOW CHARACTERISTICS OF WATER AS INFLUENCED BY CLAY CONCENTRATION

Raymond J. Miller
Allen R. Overman
John H. Peverly

Department of Agronomy
University of Illinois, Urbana

FINAL REPORT

Project No. B-002-ILL

January 1, 1966 - February 28, 1968

The work upon which this publication is based was supported by funds provided by the U.S. Department of the Interior as authorized under the Water Resources Research Act of 1964, P.L. 88-379 Agreement No. 14-01-0001-876.

UNIVERSITY OF ILLINOIS
WATER RESOURCES CENTER
3220 Civil Engineering Building
Urbana, Illinois 61801

June 1968

ABSTRACT

NON-DARCY FLOW CHARACTERISTICS OF WATER AS INFLUENCED BY CLAY CONCENTRATION

The flow of water through saturated samples of montmorillonite and kaolinite was studied to help clarify the existence and nature of non-Darcian flow. No threshold gradients were found in any of the samples studied. Non-Darcy flow was found in 9, 30 and 40 weight percent montmorillonite samples but not in a 50 weight percent montmorillonite or in kaolinite samples. The possible causes of the non-Darcian flow are discussed.

A refined technique using a pressure transducer was developed to measure hydraulic conductivities. The hydraulic conductivities of several types of samples under varying conditions were measured. Transport equations for convective diffusion in porous media were derived and tested for capillaries, porous diaphragms, sand columns and clay plugs.

Miller, Raymond J., Allen R. Overman and John H. Peverly
NON-DARCY FLOW CHARACTERISTICS OF WATER AS INFLUENCED BY CLAY CONCENTRATION
Research Report No. 16, Water Resources Center, University of Illinois, June 1968, Urbana, Illinois, v + 50 p.
DESCRIPTORS--clays/ flow/ hydraulic conductivity/ saturated flow/ saturated soils/ soil water movement/ ground water movement/ porous media/ montmorillonite/ kaolinite/ Darcy's Law/ flow characteristics/ flow rates/ flow measurement
IDENTIFIERS--Non-Darcy flow/ threshold gradients/ pressure transducers

TABLE OF CONTENTS

	Page
ABSTRACT	i
LIST OF FIGURES	iii
LIST OF TABLES	iv
LIST OF SYMBOLS	v
INTRODUCTION	1
THRESHOLD GRADIENTS AND NON-DARCY FLOW IN CLAY-WATER SYSTEMS	3
Literature Review	3
Experimental Procedures	6
Results	11
Discussion	14
HYDRAULIC CONDUCTIVITY MEASUREMENTS WITH A PRESSURE TRANSDUCER	22
Introduction	22
Description of the Pressure Transducer Method	22
Discussion	25
SOLUTE TRANSPORT BY CONVECTIVE DIFFUSION	30
Transport in Capillaries	31
Transport Through a Porous Diaphragm	35
Transport Through a Clay Plug	37
Transport Through a Sand Column	43
LITERATURE CITED	48

LIST OF FIGURES

Figure		Page
1.1	Apparatus for flow studies in saturated clays.	7
1.2	Hypothetical dissipation curves for opposite flow directions.	10
1.3	Pressure-time recorder plots for a 30 weight percent montmorillonite paste with various initial heads.	13
1.4	Log percent head versus time for the 2-20 μ kaolinite sample.	15
1.5	Log percent head versus time for the 50 weight percent montmorillonite sample.	16
1.6	Log percent head versus time for the 30 weight percent montmorillonite sample.	17
2.1	Apparatus for hydraulic conductivity measurements.	24
2.2	Transient head response for 72 weight percent kaolinite.	26
3.1	Typical graph of equation (3.4).	33
3.2	Analysis of experiment of Kemper and van Schaik (1966).	40
3.3	Analysis of experiment of Dutt and Low (1962).	41
3.4	Transient diffusion experiment for sand column.	45

LIST OF TABLES

Table		Page
2.1	Hydraulic conductivities of porous media determined by non-steady state techniques under various experimental conditions.	27
3.1	Results for porous diaphragm experiments.	38
3.2	Results for a sand column.	47

LIST OF SYMBOLS

t = time

$\bar{v}$ = velocity

∇ = gradient operator

D = diffusion coefficient

∇^2 = Laplacian operator

C = concentration

r = radial coordinate

x = axial coordinate

a = radius of capillary

ℓ = length of capillary or membrane

A = cross-sectional area

Q = volumetric flow rate

θ = Peclet number for convective diffusion

$\mathcal{L}$ = Langevin function

Q_N = net rate of solute transport

V = volume

τ = time constant

k = space coefficient for diffusion constant

λ_n = roots for transient diffusion in sand column

ϕ = volume of sand column/volume of end chamber

INTRODUCTION

Transport equations for water and solutes are fundamental to a description of rate processes in porous media. In the simplest form fluxes and driving forces are assumed to be linearly related. Such a model allows solution of a variety of boundary-value problems, transient and steady state, for both saturated and unsaturated flow. In saturated flow analytical solutions may be obtained while for unsaturated flow numerical methods are required. When proportionality between fluxes and driving forces is not observed, the transport equations are said to be nonlinear. Such factors as non-Newtonian viscosity of the permeating fluid, variations in the porous media, and nonlinear coupling of driving forces can lead to nonlinearity.

If hydraulic pressure comprises the only variable driving force, flow is said to be Darcian if the transport equation is linear, while deviations from linearity are referred to as non-Darcian flow. Two types of non-Darcian flow have been reported. In the first of these a more-than-proportional increase in flow rate occurs upon increase in the pressure gradient. In the second type, a finite gradient is required to produce flow, the yield value being referred to as a threshold gradient.

For systems in which water and solutes move in response to pressure and concentration gradients transport takes place by convective diffusion processes. Whether the transport equations are linear or nonlinear depends upon the magnitude of the Peclet number, as well as linearity of the individual transport quantities.

The present study was undertaken to further clarify the existence and nature of non-Darcian flow. A refined technique was developed for the measurement of flow properties in systems with low hydraulic conductivities. In addition, Dr. Overman conducted experiments to establish transport equations for convective diffusion in porous media.

THRESHOLD GRADIENTS AND NON-DARCY FLOW IN CLAY-WATER SYSTEMS

LITERATURE REVIEW

Darcy, in 1856, published an empirical equation relating the volume of water flow to the applied hydraulic gradient. Since that time, this simple relationship has been assumed to be valid for water flow in both saturated and unsaturated systems and has become known as Darcy's law. Some experimental evidence supports Darcy's equation, but there have been two kinds of so-called non-Darcy behavior reported in the literature. The first of these is a non-linear relationship between flow rate and gradient; as the head increases there is a disproportionate increase in flow rate. The second type of deviation is a threshold gradient, a finite gradient below which no flow occurs.

Any deviations from a simple proportionality between gradient and flow has become known as non-Darcy flow. These deviations could include changes in the properties of the fluid as well as any changes in the matrix. It may have been more meaningful and less confusing if different terms had been used for the fluid effects, i.e. Newtonian versus non-Newtonian, and the matrix effects.

Non-linear saturated flow has been found in soils by King (1898), von Engelhardt and Tunn (1954) and Hansbo (1960) and in clays by Micheals and Lin (1954), Lutz and Kemper (1959) and Miller and Low (1963). Threshold gradients have been reported for ceramic filters by Derjaguin and Krylov (1944) and for clay systems by Oakes (1960), Li (1963) and Miller and Low (1963). To account for these observations one or a combination of several

THRESHOLD GRADIENTS AND NON-DARCY FLOW IN CLAY-WATER SYSTEMS

LITERATURE REVIEW

Darcy, in 1856, published an empirical equation relating the volume of water flow to the applied hydraulic gradient. Since that time, this simple relationship has been assumed to be valid for water flow in both saturated and unsaturated systems and has become known as Darcy's law. Some experimental evidence supports Darcy's equation, but there have been two kinds of so-called non-Darcy behavior reported in the literature. The first of these is a non-linear relationship between flow rate and gradient; as the head increases there is a disproportionate increase in flow rate. The second type of deviation is a threshold gradient, a finite gradient below which no flow occurs.

Any deviations from a simple proportionality between gradient and flow has become known as non-Darcy flow. These deviations could include changes in the properties of the fluid as well as any changes in the matrix. It may have been more meaningful and less confusing if different terms had been used for the fluid effects, i.e. Newtonian versus non-Newtonian, and the matrix effects.

Non-linear saturated flow has been found in soils by King (1898), von Engelhardt and Tunn (1954) and Hansbo (1960) and in clays by Micheals and Lin (1954), Lutz and Kemper (1959) and Miller and Low (1963). Threshold gradients have been reported for ceramic filters by Derjaguin and Krylov (1944) and for clay systems by Oakes (1960), Li (1963) and Miller and Low (1963). To account for these observations one or a combination of several

explanations is usually invoked. These are: (1) quasi-crystalline water; (2) particle reorientation; (3) electrokinetic effects and (4) a range in pore sizes.

Von Engelhardt and Tunn, Hansbo, Lutz and Kemper, and Miller and Low accounted for the non-linearity they observed by invoking the idea that clay surfaces alter water structure. This altered water is thought to be more ordered because of surface-induced hydrogen bonding and is most pronounced at the clay-water interface. The amount of hydrogen-bonded water decreases with distance from the clay surface until normal water is reached. The distance to normal water depends on the surface, its charge, and the exchangeable ions present. When low heads are applied, water flows in the center of the pores only, where the least-altered water exists. With each higher pressure increment, additional layers of water are sheared, giving increased permeabilities or flow rates. This continues with further increases in head until the whole pore is conducting water.

Low (1961) has suggested that the presence of a threshold gradient would be a critical test for the presence of quasi-crystalline water on clay surfaces. Below the threshold, no water would flow and thus electroviscous or plugging effects could be discounted. Miller and Low (1963) argued that if clay surfaces do order water, then at some clay concentration this quasi-crystalline water would extend across the entire pore. A finite energy, or head, would be needed to break down this structured barrier before flow would begin. On the basis of the threshold gradient they reported and from experiments which indicated that the activation energy for water

flow in clay pastes increased as the applied gradient decreased, Miller and Low concluded that a quasi-crystalline water structure does exist on clay surfaces.

Micheals and Lin (1954), Martin (1962) and Mitchell and Younger (1967) suggest that particle reorientation is the most important effect in non-Darcy flow. These matrix effects need not be just a simple movement of particles, but may include bending and flexing of particles or the breaking of edge-to-surface bonds to permit particle orientation with the flow path.

Micheals and Lin (1955) postulated an electroviscous resistance to flow which decreased with increasing head, as the flow restricting cations were swept into the larger pores. Kemper (1960) suggested a similar mechanism. However, Micheals and Lin concluded that these effects were probably small. Since electrokinetic theory and experimental results suggest that there is a linear relationship between the electroviscous effect and applied pressure, this factor is probably not of major importance.

Miller and Low suggested that non-linear flow could be caused by a range in pore size. As the hydraulic gradient was increased, the threshold gradient was exceeded in smaller pores increasing the flow rate. A threshold gradient is necessary for this explanation.

Portions of the above non-Darcy data have been criticized for various reasons. Li's (1963) data was questioned by Olsen (1965) because of uncorrected experimental errors which could account for the reported threshold gradients. Oakes (1960) cited only one of several experiments in which

threshold gradients were found. Since no experimental details were given, it is possible that evaporation and other errors weren't compensated for. Jackson (1967) contends that the threshold gradient that Derjaguin and Krylov (1944) observed in ceramics was a result of osmotic effects. Olsen (1965) has shown that air-contaminated capillaries could account for some of the non-Darcy and threshold gradient characteristics reported. Hansbo's reported deviations can be entirely accounted for this way, and the data of von Engelhardt and Tunn, Miller and Low, and Lutz and Kemper can be partially discredited on this basis.

It is clear that the question of the existence of general non-Darcy behavior and specifically threshold gradients for water flow in saturated clay systems is unanswered. Therefore, flow studies were conducted in concentrated Wyoming bentonite and kaolinite clay samples. The existence of the threshold gradient was tested for specifically in these clay-water systems.

EXPERIMENTAL PROCEDURE

Figure 1.1 shows the glass flow cell and other apparatus used to test for a threshold gradient in clay-water pastes. Fine or coarse fritted glass disks, 2 cm in diameter and 2 mm thick were used to confine the clay. One frit, F_1, was fused into a pyrex glass tube, the other frit, F_2, being fused into the ball end of a glass ball and socket joint, J, so as to form a flow cell 2.5 cm long.

The head drop across the flow cell was monitored continuously with a Pace model KP15 differential pressure transducer, with a $\pm$1psi linear-

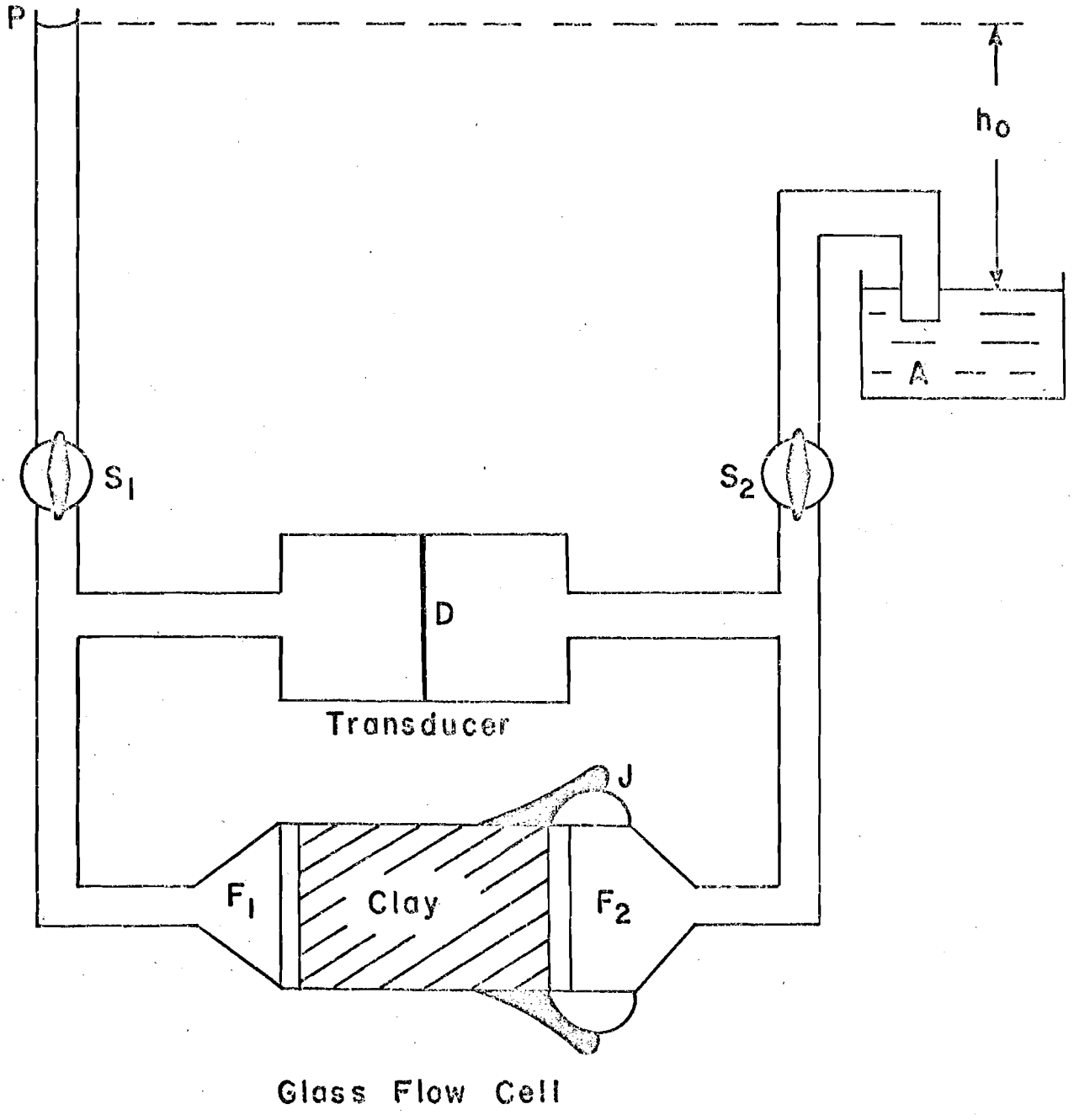

Figure 1.1 Apparatus for flow studies in saturated clays.

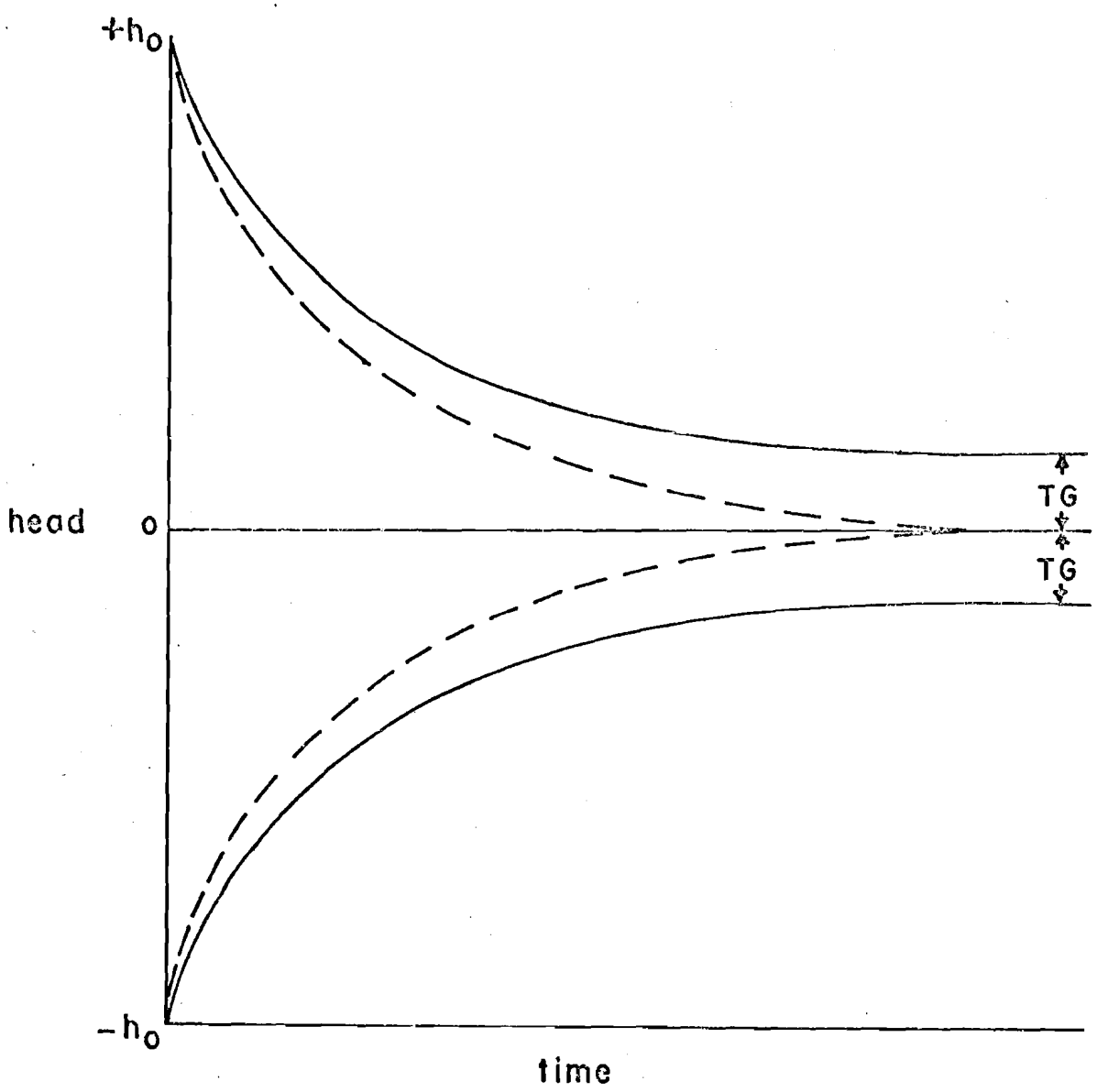

Figure 1.2. Hypothetical pressure dissipation curves for opposite flow directions. Initial heads $+h_o$ and $-h_o$ referring to heads applied to the right and left sides of the apparatus, respectively. Solid line, threshold gradient, TG. Dashed line, no TG.

There was a displacement of the zero line as previously described in all montmorillonite samples, but not in the kaolinites. This was attributed to osmotic forces and would have no effect on threshold gradient measurements.

Figure 1.3 shows typical pressure-time recorder plots for the 30 weight percent montmorillonite sample using initial heads of 5, 20, 50 and 100 cm H_2O. There was no indication that various heads had different effects on flow behavior in any of the samples. Similar results were obtained for all samples studied.

If Darcy's law is applicable to non-steady state flow as well as to steady state flow, then data of the type shown in Figure 1.3 can be used to study the flow properties of these systems. The volumetric flow rate Q, and the pressure head h, are related by Darcy's law

$$Q = \frac{KA}{\ell} \quad h \tag{1.1}$$

where A is the cross-sectional area of the flow cell, ℓ is the length of the porous media and K is the hydraulic conductivity. The transducer's volumetric discharge, Q, is given by

$$Q = -\frac{dV}{dt} = -\frac{dV}{dh}\,\frac{dh}{dt} = -\alpha\frac{dh}{dt} \tag{1.2}$$

where t is any time and $\alpha = \frac{dV}{dh}$, the transducer volumetric displacement factor. The combination and integration of equations (1.1) and (1.2) results in

$$\ln \frac{h - h_\infty}{h_o - h_\infty} = -t\,\frac{\ell\alpha}{AK}$$

where h_o and h_∞ are the initial and final pressure heads respectively. Semilog plots of $\frac{h - h_\infty}{h_o - h_\infty}$ versus time should be linear if K is constant.

diaphragm's equilibrium position. If there is a threshold gradient, flow will stop when the threshold value is reached, as indicated by the solid curves in Figure 1.2. At this point diaphragm movement towards the equilibrium position will stop. The magnitudes of the plateaus will be equal from both flow directions.

Montmorillonites are unstable even in water and decompose releasing salts into solution. Such decomposition, or contamination of apparatus, can result in unexpected osmotic effects. That such potentials are important in porous media has been shown by Low (1955) and Jackson (1967). These effects can be tested for by placing equal heads on both sides of the diaphragm, closing both stopcocks and recording the output. If there are no osmotic effects, the transducer output will not change. If there are osmotic effects, water will move toward the greater salt concentration, generating a pressure, and hence, changing the recorder signal. The stable osmotic pressure generated is then taken as the new zero line, with no effects on threshold gradient determinations. The percent head, h/h_o, can be calculated by adding or subtracting the osmotic pressure depending on the horizontal flow direction. The new osmotic zero line will change over extended times, because the clay plug is not a perfect semipermeable membrane. For the times involved in these experiments, the osmotic zero line was essentially constant. If flow studies are initiated and any osmotic effects present are not accounted for, apparent threshold gradients can be found.

RESULTS

No threshold gradient was found in any of the clay pastes tested. Over the temperature range of 5 to 30°C, all pressure-time recorder plots, from either direction, dissipated to one percent or less of the applied head.

There was a displacement of the zero line as previously described in all montmorillonite samples, but not in the kaolinites. This was attributed to osmotic forces and would have no effect on threshold gradient measurements.

Figure 1.3 shows typical pressure-time recorder plots for the 30 weight percent montmorillonite sample using initial heads of 5, 20, 50 and 100 cm H_2O. There was no indication that various heads had different effects on flow behavior in any of the samples. Similar results were obtained for all samples studied.

If Darcy's law is applicable to non-steady state flow as well as to steady state flow, then data of the type shown in Figure 1.3 can be used to study the flow properties of these systems. The volumetric flow rate Q, and the pressure head h, are related by Darcy's law

$$Q = \frac{KA}{\ell} \quad h \tag{1.1}$$

where A is the cross-sectional area of the flow cell, ℓ is the length of the porous media and K is the hydraulic conductivity. The transducer's volumetric discharge, Q, is given by

$$Q = -\frac{dV}{dt} = -\frac{dV}{dh}\,\frac{dh}{dt} = -\alpha\frac{dh}{dt} \tag{1.2}$$

where t is any time and $\alpha = \frac{dV}{dh}$, the transducer volumetric displacement factor. The combination and integration of equations (1.1) and (1.2) results in

$$\ln \frac{h - h_\infty}{h_o - h_\infty} = -t\,\frac{\ell\alpha}{AK}$$

where h_o and h_∞ are the initial and final pressure heads respectively. Semilog plots of $\frac{h - h_\infty}{h_o - h_\infty}$ versus time should be linear if K is constant.

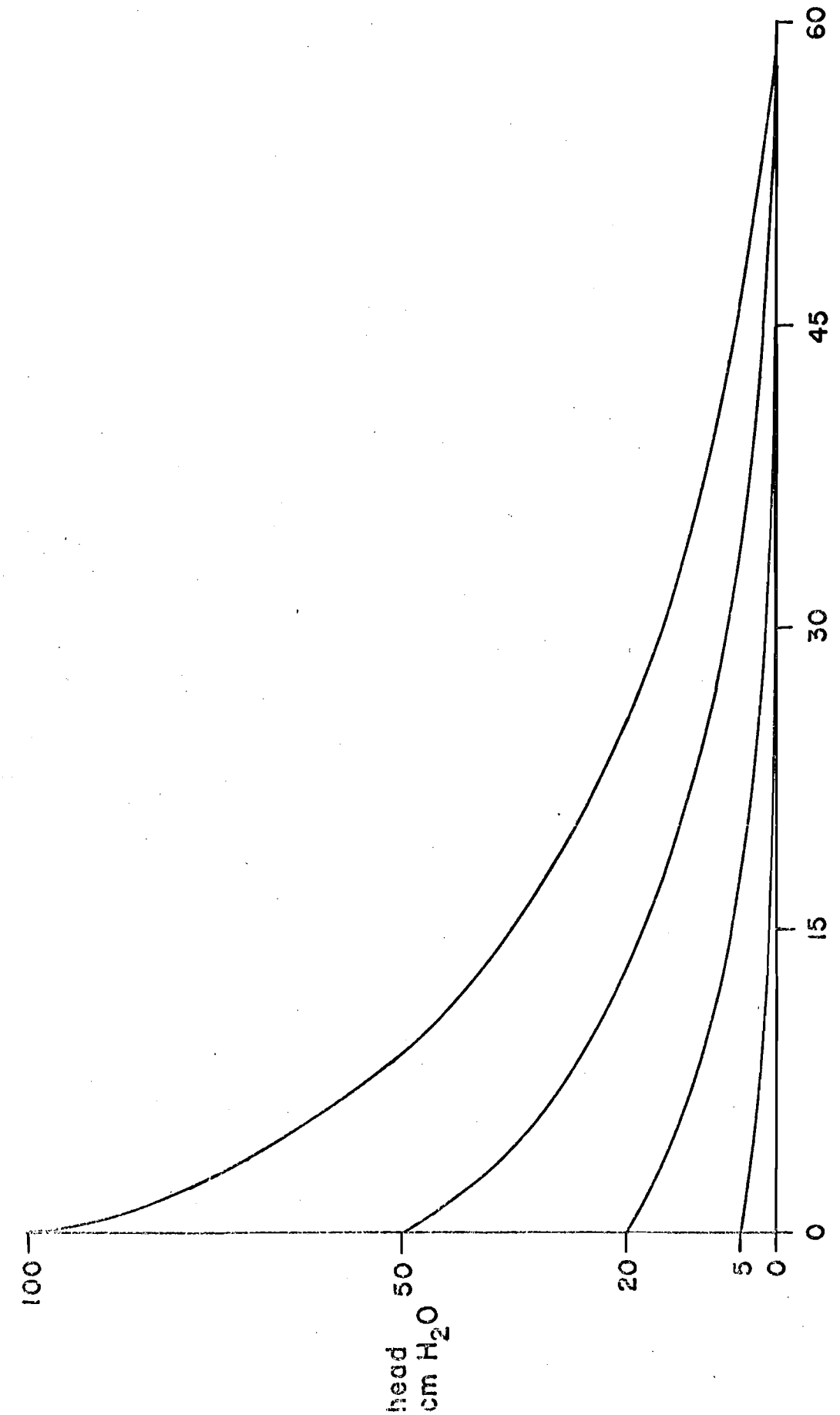

Figure 1.3. Pressure-time recorder plots for a 30 percent montmorillonite paste with various initial heads.

Semilog plots for both kaolinite samples, Figure 1.4, and for the 50 percent montmorillonite sample, Figure 1.5, were linear. The 9, 30 and 40 weight percent montmorillonite samples showed initial curvilinearity in the semilog plots, but become linear after approximately 40 percent of the initial head, h_o, had dissipated (Figure 1.6).

DISCUSSION

In the systems tested no threshold gradients were found. The water in these systems is not stabilized by the clay surfaces to the extent that a finite pressure is needed to cause the water to flow. The water retains fluid properties at all clay concentrations.

Of the threshold gradients reported in the literature, Miller and Low (1963) were the only ones to present experimental detail and data. Of the four systems they tested, three had negative or reverse flow at zero gradient. This was probably a result of osmotic forces (Jackson, 1967; Low, 1955). Even though Miller and Low corrected for the reverse flow, 2 of these 3 samples showed a threshold gradient. The flow at zero head makes the threshold gradient observed in these two cases questionable. The fourth sample, 55.5 weight percent montmorillonite, had the highest threshold gradient and no flow at zero head. Why a threshold gradient was observed in their sample and not in the 50 weight percent montmorillonite sample tested in this work is not known.

It can be argued that because the 30, 40 and 50 percent clays prepared for this experiment had no hydrous aluminum oxide film on the surface, as did those of Miller and Low (1963), the threshold gradient

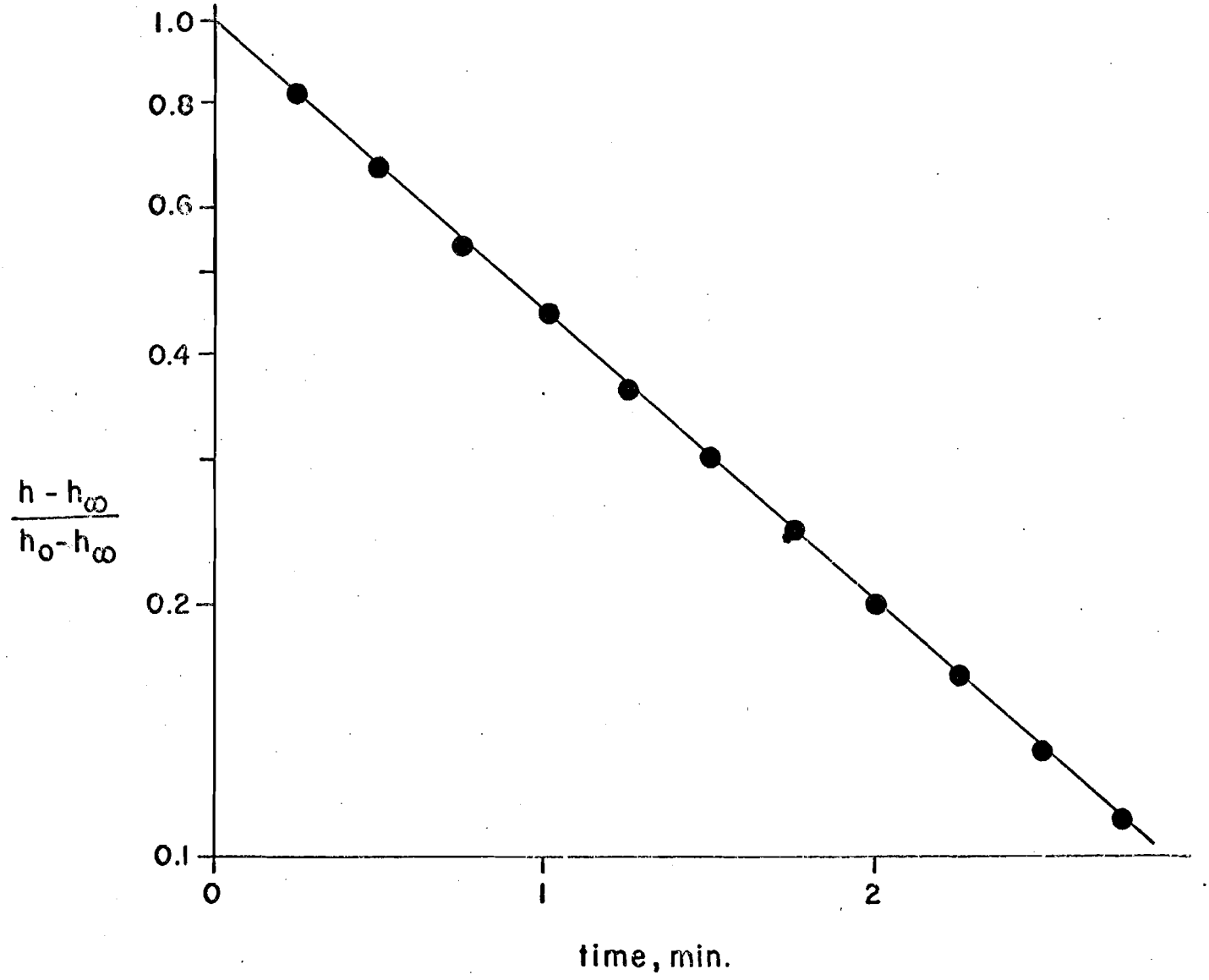

Figure 1.4. Log percent head versus time for the 2-20 kaolinite sample. h_o = 50 cm H_2O.

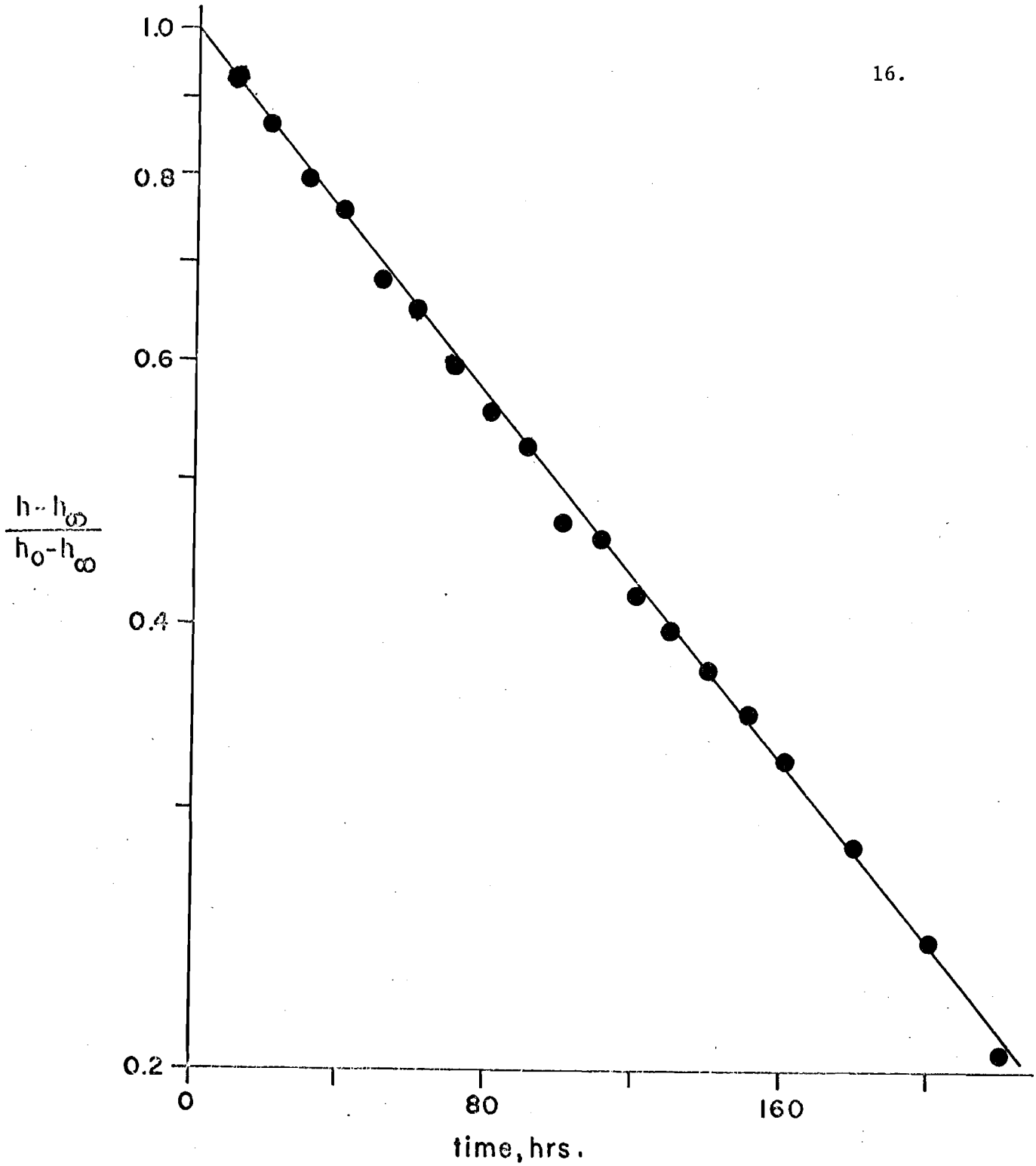

Figure 1.5. Log percent head vs time for the 50 percent montmorillonite sample. h_o = 200 cm H_2O.

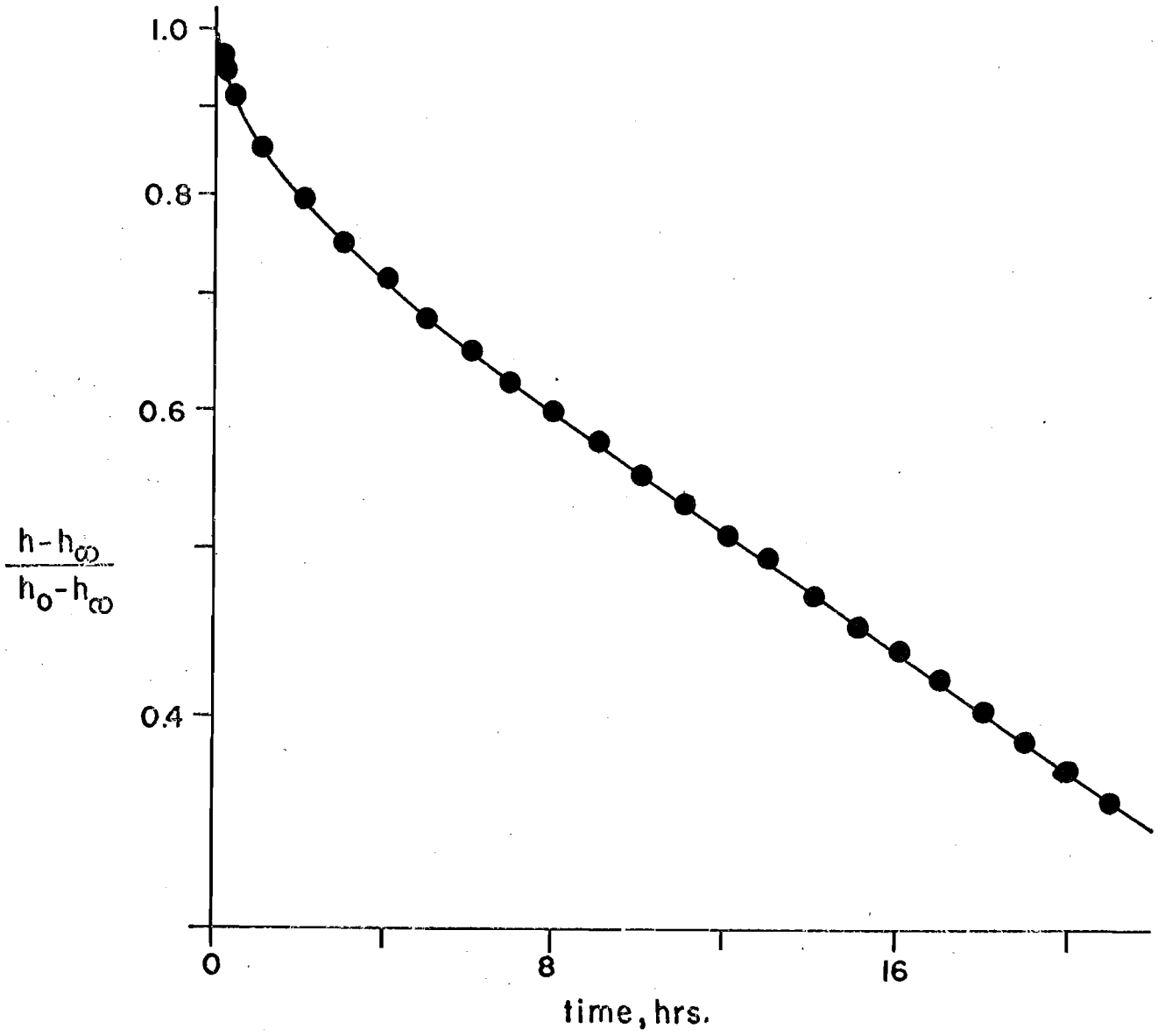

Figure 1.6. Log percent head vs time plot for the 30 percent montmorillonite sample. Similar semilog plots were obtained for the 9 and 40 percent montmorillonite samples. h_o = 50 cm H_2O.

observed by them was a result of such a film. The evidence is incomplete on this point.

Before discussing the semilog plots of Figures 1.4, 1.5, and 1.6 and their interpretation, the characteristics of the two clays used should be remembered.

Kaolinite is a 1:1 layer silicate with the individual platelets held together by hydrogen bonding, forming packets of various sizes. This is a non-expanding clay. When a size of $<2\mu$ is quoted, it only means that it is less than 2μ assuming equivalent spherical dimensions. Kaolinite has a small surface area because of the stacking of plates. Montmorillonite, on the other hand, is a 2:1 layer silicate with expanding characteristics. Montmorillonite, when saturated with sodium or lithium, is not considered to exist in packets of more than a few (1-6) individual plates. Because it is an expanding mineral, it has a large surface area.

Because of its characteristics montmorillonite would be expected to be more subject to matrix rearrangements. It will have a large component of particles that can bend, flex and move, whereas kaolinites do not have many small particles to move or shift. Similarly, because of their low surface area, kaolinites are usually thought of as minimizing water structure effects. The kaolinite's effect will be as large per unit of area but since there is so little area the water effects would be hard to measure. Montmorillonite, having both a large surface area and associated exchange capacity, would be expected to maximize any water effect that is a result of surface or charge induced phenomena.

As discussed in the literature review, four explanations have been suggested to account for changes in flow rate with changes in head (Figure 1.6).

Since no threshold gradients were found, the effects of varying pore sizes can be eliminated. The only two hypotheses that will be discussed are: matrix effects and a quasi-crystalline water structure resulting in shear-dependent viscosities.

Recall that for the 2 kaolinites and the 50 percent montmorillonite, straight line semilog plots were obtained, Figures 1.4 and 1.5. For the 9, 30, and 40 percent montmorillonite samples, the semilog plots were curvilinear, Figure 1.6. Water movement in the first 3 clays obeys Darcy's law but in the latter 3 clays it does not. From the above discussion, it would be expected that if non-Darcy behavior is a result of either water or matrix effects they would not be expected in the kaolinite samples but would be in the montmorillonite samples. Except for the 50 percent montmorillonite sample, the semilog plots bear this out.

To explain the 50 percent data, the effects of high clay concentrations can be invoked. As the montmorillonite sample becomes more concentrated the particles are in closer proximity and the swelling pressure between the particles increases. At some clay concentration, apparently above 40 percent, these forces could become great enough to stabilize the particles, preventing or reducing matrix effects at the low flow rates used. When 50 weight percent is reached, no particle rearrangement takes place or it is so slow that Darcian flow results as borne out by the linear semilog plot.

If the water in the vicinity of clay is quasi-crystalline the closer the particles are together the greater the proportion of ordered water. If movement of different layers of this water is shear dependent, the greater the clay concentration, the greater the non-Darcy flow. The 30

and 40 percent samples would tend to support this argument, but not the 50 percent sample. It is possible that when the particles are this close together (25 A), the force fields are so great that water structure is destroyed and Darcy flow characteristics appear again.

Which of these two possibilities is most likely is not clear. It would seem that, in many of the experiments where non-Darcy flow has been reported, either the samples or the method used would be conducive to particle rearrangement.

Why curvilinearity was found only in the initial portion of the semilog plots and became linear at about 40 percent pressure dissipation for the 9, 30 and 40 percent montmorillonites is not clear. No evidence indicating a pressure dependent relaxation of the containing cells could be found. How matrix or water structure effects could cause the pressure dissipation rate to become linear with the same percentage pressure remaining in the different samples is not obvious.

The pressure dissipation with time (Figure 1.6) in the 30 weight percent montmorillonite samples behaved as the boundary value problem for diffusion. This suggested that the pressure transfer was by diffusive processes. If it is assumed that all of the water transport is diffusive, a diffusion coefficient, D, can be calculated using equation (1.3),

$$Q = \frac{DA}{\ell} \frac{\rho g}{RT} h \qquad (1.3)$$

where ρ is the density of water, g is the acceleration due to gravity, T is the absolute temperature and R is the gas constant. The calculated

diffusion coefficient is 1×10^{-3} cm^2/sec which is approximately two orders of magnitude greater than that for the diffusion of water in normal water. Hence, this is not a diffusion controlled process.

Threshold gradients below which no flow occurred were not found in any of the samples tested. Non-Darcy flow was observed in 9, 30 and 40 weight percent montmorillonite sample but not in the 50 weight percent montmorillonite sample or either of the kaolinite samples. This non-Darcy flow could be caused by matrix effects or surface induced water structure.

HYDRAULIC CONDUCTIVITY MEASUREMENTS WITH A PRESSURE TRANSDUCER

INTRODUCTION

Measurements of the permeability of soils or clays may be steady-state or transient-state (Klute, 1965). In the steady-state method, values are obtained for the set (Q, h), where h is the applied differential pressure head and Q is the volumetric flow rate. Measurement of Q is generally obtained by following the movement of an air bubble in a capillary tube (Miller and Low, 1963). This method can lead to erroneous results due to contaminated capillaries (Olsen, 1965). In studies with kaolinites, Olsen (1966) avoided this problem by using a syringe pump to control Q. With the transient-state method the set (h, t) is monitored, where t is the time. Values of h are obtained from piezometers. Response time is inversely related to the bore of the standpipes, and for systems of low conductivity may become too long to obtain meaningful data. Employment of a pressure transducer with low volume displacement can overcome this problem.

DESCRIPTION OF THE PRESSURE TRANSDUCER METHOD

The permeameter and pressure transducer are assembled as shown in Figure 2.1. A differential water head of h cm of H_2O is applied, which displaces the diaphragm within the transducer. Upon closing the stopcock, this head dissipates with time due to transfer of water through the permeameter. By measuring the voltage output of the transducer, a record of head with time is obtained.

The set (Q, h) is assumed related by Darcy's law

$$Q = \frac{KA}{\ell} h \tag{2.1}$$

where K is the hydraulic conductivity, A the cross-sectional area of the permeameter, and ℓ the length of the soil column. Volumetric discharge of the transducer is given by

$$Q = - \frac{dV}{dt} = - \alpha \frac{dh}{dt} \tag{2.2}$$

where $\alpha = \frac{dV}{dh}$, the volumetric displacement factor of the transducer, is a constant for heads less than h_o. Solution of the system of equations (2.1) and (2.2) yields

$$\frac{h - h_\infty}{h_o - h_\infty} = e^{- t/\tau} \tag{2.3}$$

where h_o and h_∞ are the initial and final pressure heads respectively, and $\tau = \ell\alpha/AK$ is the time constant of the system.

Analysis of the data from a 72 weight percent saturated kaolinite[2] illustrates this technique. The clay was the 2-20 μ size fraction with 60 percent in the 2-10 μ range. A pace model KP15 differential pressure transducer, $\pm$ 1 psi diaphragm, was connected as shown in Figure 2.1. Transducer output was provided by a Pace model CD10 carrier-demodulator. The dc voltage was applied to a 1:100 voltage divider to obtain a millivolt signal suitable for a Sargent model SR recorder. The voltage signal was then attenuated so that h = 50 cm H_2O corresponded to 100 percent on the chart paper, while h = 0 cm H_2O corresponded to 0 percent. After applying h_o, the teflon stopcock was closed and recording begun. After five minutes

[2]Minerals and Chemicals Philipp Corporation, Menlo Park, N.J.

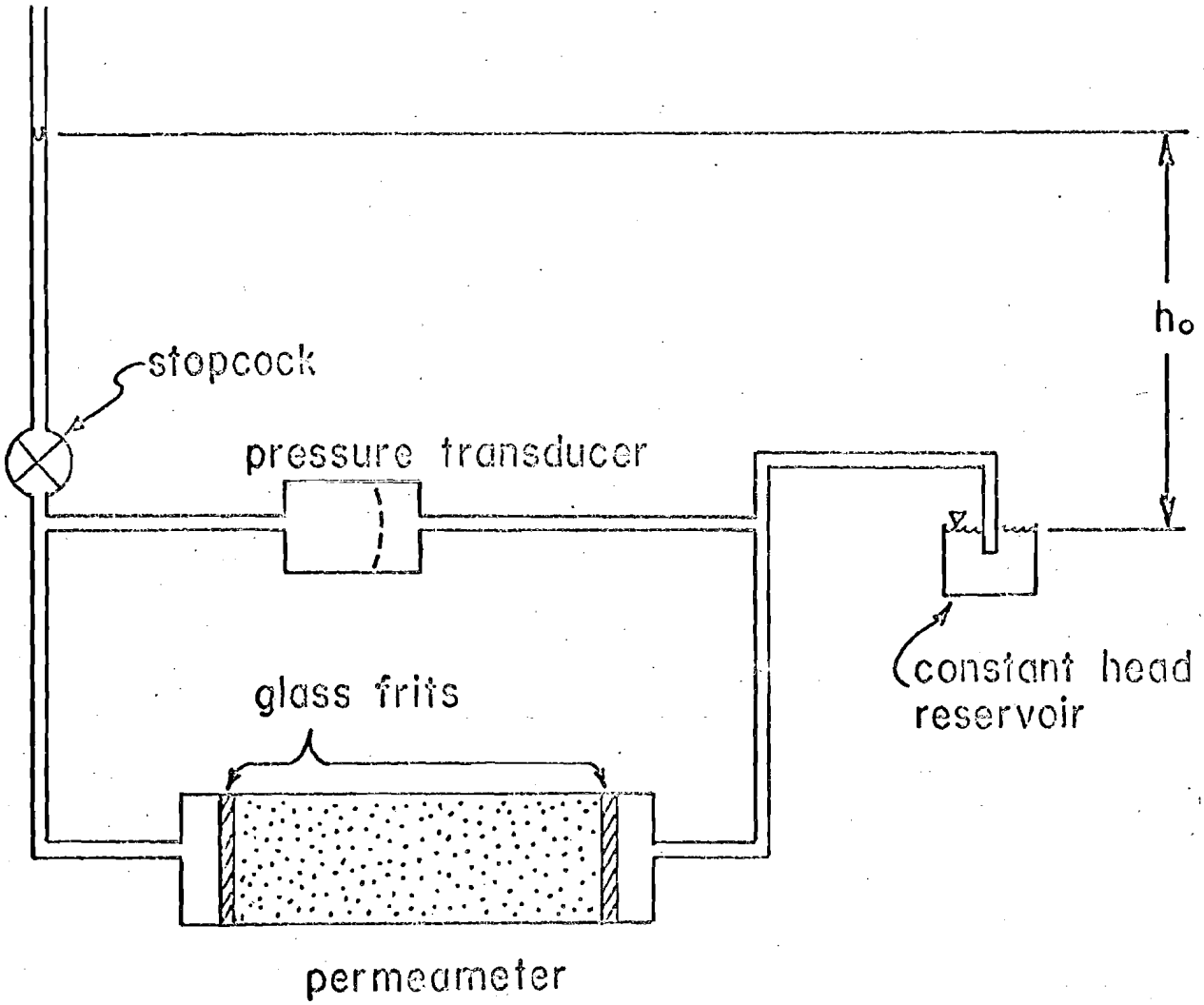

Figure 2.1. Apparatus for hydraulic conductivity measurements.

the pressure head had essentially reached its final value. Readings from the chart are shown in Figure 2.2, where $h_o = 50$ and $h_\infty = 0$. A regression analysis with $-\ln h/h_o$ as the dependent variable and time the independent variable resulted in $\tau = 1.214 \pm 0.006$ at the 95% confidence level. The solid line in Figure 2.2 is the regression line. A clay column of 2.0 cm diameter, 2.4 cm long, and $\alpha = 1.10 \cdot 10^{-4}$ $cm^3/cm\ H_2O$, resulted in a calculated hydraulic conductivity $K = 1.16 \cdot 10^{-6}$ cm/sec. This value is intermediate to that of Olsen (1966) and the value of Micheals and Lin (1954) for kaolinite of the same concentration but from different sources.

DISCUSSION

It was shown above how use of a pressure transducer can reduce the time constant for measuring hydraulic conductivity. Results, Figure 2.2, using kaolinite, where $K \approx 10^{-6}$ cm/sec indicate the potential of the method. This technique has been used with a number of materials and experimental conditions. The results are summarized in Table 2.1. In general, there is a decrease in conductivity with increasing clay concentration and with decreasing temperature and particle size. Varying the initial gradient does not change the conductivity. The values are comparable to values obtained previously by other methods (Micheals and Lin, 1954; Miller and Low, 1963; Olsen, 1966).

The semilog plots of $\frac{h - h_\infty}{h_o - h_\infty}$ versus t for the 9, 30, and 40 weight percent montmorillonites were not linear, but were curvilinear until approximately 40 percent of the head had dissipated, after which the plot

Figure 2.2. Transient head response for 72 weight percent kaolinite.

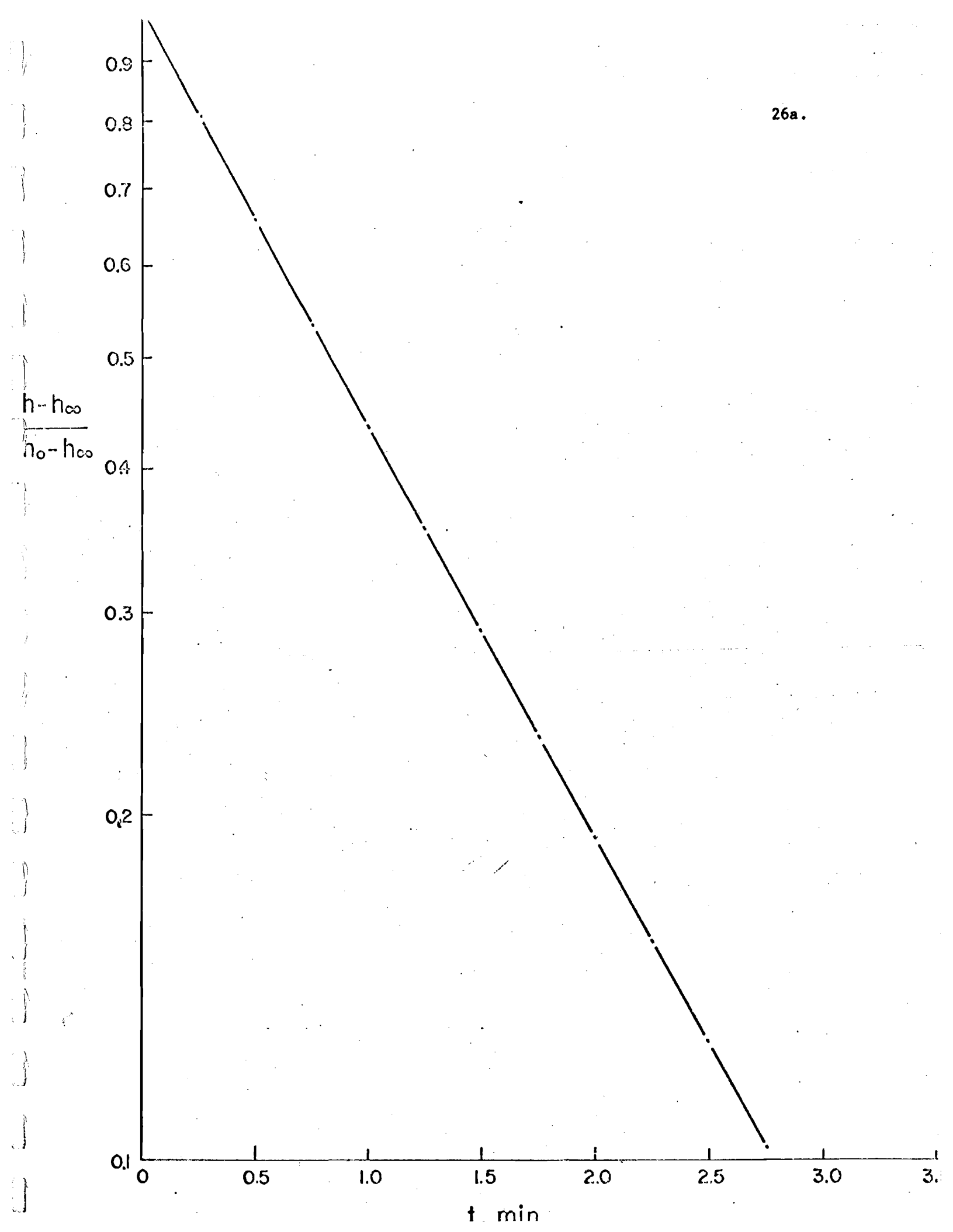
0.9
0.8
0.7
0.6
0.5
h-h∞ / h₀-h∞
0.4
0.3
0.2
0.1
0
0.5
1.0
1.5
2.0
2.5
3.0
3.
t min

Table 2.1 Hydraulic conductivities of porous media determined by non-steady state techniques under various experimental conditions.

Sample Material	Per Cent By Weight	Particle Size, μ	Temperature Degrees C	Hyd. Cond. 10^{-7} cm/sec	Initial Gradient H_2O
Glass beads	packed	150-175	23.0	4522.*	20.0
Kaolinite	72.5	2-20	30.0	15.*	20.0
"	72.5	< 2	30.0	11.	20.0
Kaolinite	81.1	< 2	30.0	1.94	10.0
"	81.1	< 2	30.0	1.96	20.0
"	81.1	< 2	30.0	1.98	30.0
Na/Al mont.	9.64	< 2	5.9	.096	1.4
Na-satrd. mont.	30.	< 2	16.0	.0091	8.0
"	30.	< 2	16.0	.0092	20.0
"	30.	< 2	16.0	.0093	40.0
Na-satrd. mont.	35.8	< 2	18.2	.0014	10.0
Na-satrd. mont.	40.	< 2	31.1	.0056	20.0
"	40.	< 2	14.3	.0045	80.0
Na-satrd. mont.	50.	< 2	30.8	.0015	80.0

*Indicates that the conventional falling head-standpipe method was used as opposed to the stopcock-diaphragm method.

was linear. The cause of the nonlinearity is not known. Hydraulic conductivities were calculated using the linear part of the plot. These values agreed well with those of Miller and Low (1963). For the montmorillonite systems, estimates of h_∞ become important (Jackson, 1967) and are more difficult to make because of the longer time constants.

Since the system described is sensitive to small volume transfer, several precautions must be taken in its use. These are: (1) linearity of voltage with pressure input; (2) constancy of the volumetric displacement factor, α; (3) absence of leaks; (4) small expansion of any joints with pressure; and (5) temperature control.

For the transducer used in this study linearity was better than 1 percent as shown by applying known heads and measuring the output. A number of commercial systems are available with this level of precision.

Constancy of α for the Pace transducer ($\pm$1 psi diaphragm) was established by connecting a precision bore capillary to one side of the transducer and applying known heads to the opposite side. A meniscus in the capillary was found to displace linearly with head up to 50 cm H_2O, but exhibited nonlinearity beyond this range.

Leakage may be tested by closing the right side of the permeameter, Figure 2.1, and applying a head to the left side. Upon closing the stopcock, this pressure head will be maintained with time if no leaks are present.

Expansion of joints can be troublesome by overshadowing the displacement factor, α, of the transducer. The extent of expansion may be determined by disconnecting the right side of the transducer, Figure 2.1,

SOLUTE TRANSPORT BY CONVECTIVE DIFFUSION

INTRODUCTION

In this discussion solute transport will be treated within the framework of continuum mechanics rather than molecular, or statistical, mechanics. This approach naturally gives rise to the well known continuity, or mass balance, equation (cf Cole, 1962). Only two driving potentials will be considered, viz., gradients of concentration and pressure. Furthermore, adsorption and chemical reaction will be excluded from the treatment.

In our context, solutes move through a porous system by two processes. First, if the solution is flowing relative to the solid boundary, then transport occurs by convection, solute flux being controlled simply by the flux of solution and the solute concentration within the solution. Second, concentration differences within the solution give rise to diffusion, the system tending toward uniform concentration throughout.

For higher flow rates the diffusive exchange is enhanced and the overall process is referred to as dispersion. The so-called dispersion coefficient is observed to increase as solution flux increases. With diminishing flow rate the dispersion coefficient degenerates to the molecular diffusion coefficient. As these studies clearly show, solute transport is then described by the linear superposition of the diffusion and convection equations. It will be seen, however, that the difference form of Fick's first law may be employed only under rather limited conditions. This restriction arises from the general nonlinearity of the concentration profile.

Mathematically, the effect of convection is to replace the temporal derivative $\partial/\partial t$ in the continuity equation by the material derivative $D/Dt = \partial/\partial t + v \cdot \nabla$. The significance of these two forms is discussed by Bird, Stewart, and Lightfoot (1960). When the solution remains fixed in the coordinate frame, the two are synonymous.

Physically, the net result of diffusion and convection depends upon the direction and magnitude of each. When the two are parallel net flux of solute is enhanced, whereas, net flux is reduced when the two are anti-parallel. As mentioned above, there is an interaction due to influence of convection on the concentration gradient.

Attention is first focused on flow through cylindrical capillaries, due to their geometric simplicity. The treatment is then extended to porous media such as porous diaphragms and packed columns.

TRANSPORT IN CAPILLARIES

The continuity equation for convective diffusion is

$$D \nabla^2 C = \frac{\partial C}{\partial t} + v \cdot \nabla C \qquad (3.1)$$

Definitions of the terms may be found at the beginning of this report. By assuming radial symmetry for concentration and velocity, constancy of the diffusion coefficient, and Poiseuille's equation for velocity distribution, Taylor (1953) gives

$$D \left(\frac{\partial^2 C}{\partial r^2} + \frac{1}{r} \frac{\partial C}{\partial r} + \frac{\partial^2 C}{\partial x^2} \right) = \frac{\partial C}{\partial t} + V_o \left(1 - \frac{r^2}{a^2} \right) \frac{\partial C}{\partial x} \qquad (3.2)$$

for the continuity equation. Overman (1965) simplified equation (3.2) by neglecting the radial component of the Laplacian and by replacing the parabolic velocity term by an average velocity $\bar{v}$, which reduces the problem to one of axial transport. Equation (3.2) then becomes

$$D \frac{\partial^2 C}{\partial x^2} - v \frac{\partial C}{\partial x} - \frac{\partial C}{\partial t} = 0 \qquad (3.3)$$

Consider the steady-state case, first. With the boundary conditions $C(x=0) = C_o$ and $C(x=\ell) = C_\ell$, the solution to equation (3.3) is

$$\frac{C - C_\ell}{C_o - C_\ell} = 1 - \frac{e^{\theta x/\ell} - 1}{e^{\theta} - 1} \qquad (3.4)$$

where $\theta = \ell v/D = \ell Q/DA$ is the Peclet number. The behavior of equation (3.4) is shown in Figure 3.1. For pure diffusion equation (3.4) becomes linear, consistent with the solution of the diffusion equation. Average concentration of solute in the capillary is given by

$$\frac{\bar{C} - C_\ell}{C_o - C_\ell} = \frac{1}{2} \left[1 + \mathcal{L}\left(\frac{\theta}{2}\right) \right] \qquad (3.5)$$

where $\mathcal{L}(z) = \coth z - 1/z$ is the Langevin function. The applicability of equation (3.5) to data obtained with $D_2O - H_2O$ has been confirmed in a paper by Overman and Miller (1968). Agreement between theory and experiment was within 2 percent for a Peclet number of 3.88. The known value for the diffusion coefficient of $D_2O - H_2O$ was used.

The transient solution to equation (3.3), subject to the boundary and initial conditions $C(0,t) = C_o$, $C(\ell,t) = C_\ell$, and $C(x,0) = C_o$, has been

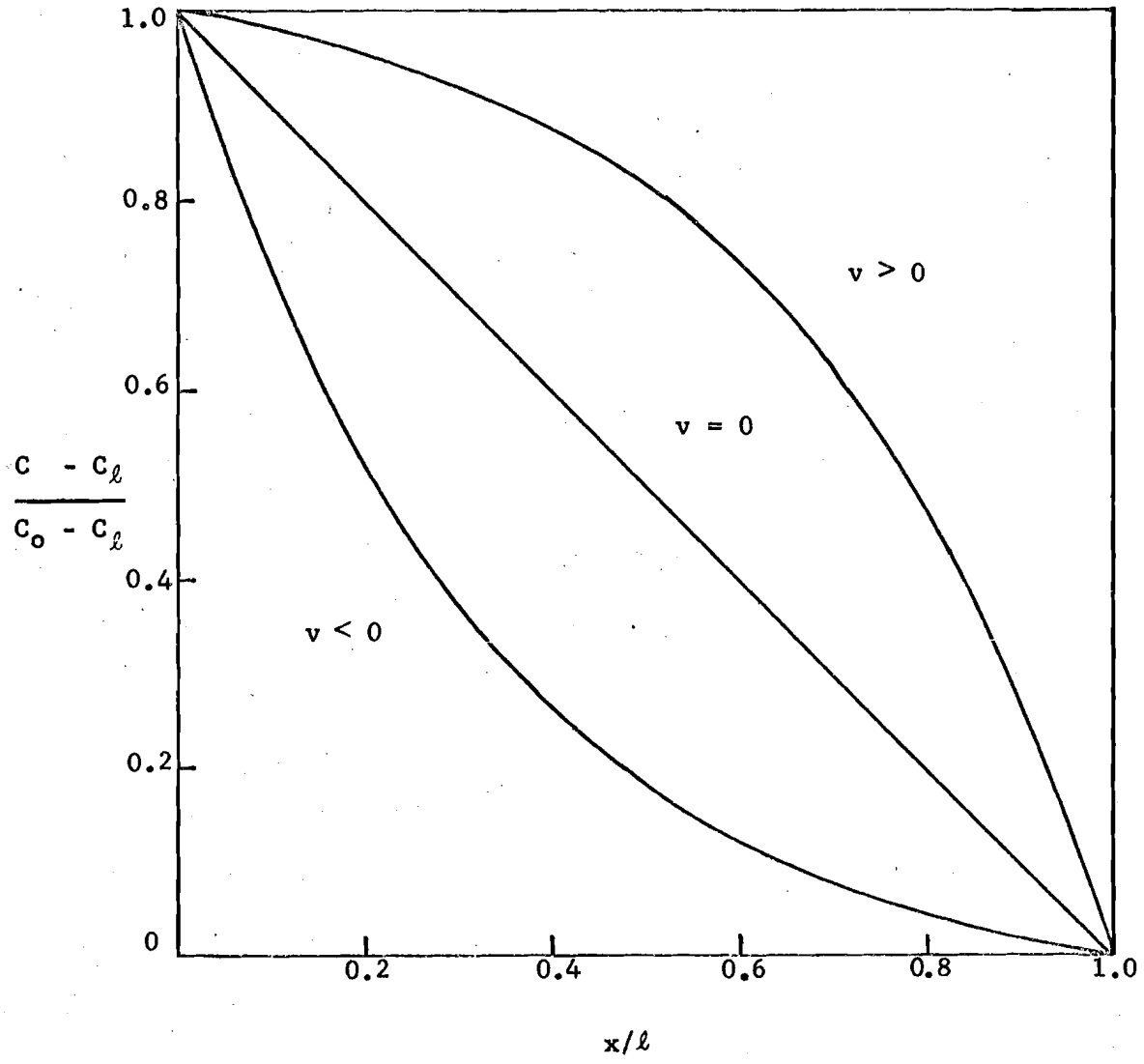

Figure 3.1. Typical graph of equation (3.4).

obtained by Overman (1968a) in the form

$$\frac{C - C_\ell}{C_o - C_\ell} = 1 - \frac{e^{\theta x/\ell} - 1}{e^{\theta} - 1}$$

$$-2\, e^{-\frac{\theta}{2}(1-x/\ell)} \sum_{n=1}^{\infty} \frac{n\pi \cos n\pi}{\frac{\theta^2}{4} + n^2\pi^2}\, e^{-\left|\frac{\theta^2}{4} + n^2\pi^2\right| \frac{Dt}{\ell^2}} \sin n\pi \frac{x}{\ell} \qquad (3.6)$$

In the limit $t \to \infty$ equation (3.6) reduces to equation (3.4). Average concentration is now given by

$$\frac{\bar{C} - C_\ell}{C_o - C_\ell} = \frac{1}{2}\left[1 + \mathfrak{L}\left|\frac{\theta}{2}\right|\right]$$

$$+ 2 \sum_{n=1}^{\infty} \left(\frac{n\pi}{\frac{\theta^2}{4} + n^2\pi^2}\right)^2 (1 - e^{-\frac{\theta}{2}} \cos n\pi)\, e^{-\left(\frac{\theta^2}{4} + n^2\pi^2\right) \frac{Dt}{\ell^2}} \qquad (3.7)$$

Again in the limit $t \to \infty$, equation (3.7) reduces to equation (3.5). Measured values agreed with those predicted by equation (3.7) to within 2 percent for a Peclet number of 3.88. Discrepancies probably occur for small t due to neglect of the radial component of the Laplacian operator.

These results suggest that net transfer of solute is adequately described by

$$Q_N = -DA \frac{dc}{dx} + QC \qquad (3.8)$$

at steady state. The integral form of the transport equation

$$Q_N = Q \frac{C_o e^{\theta} - C_\ell}{e^{\theta} - 1} \qquad (3.9)$$

is obtained by combining equations 3.4 and 3.8. Two special cases follow:

$$Q_N = Q C_o \qquad C_o = C_\ell \qquad (3.10)$$

$$Q_N = DA \frac{C_o - C_\ell}{\ell} \qquad \theta = 0 \qquad (3.11)$$

as expected. In general, equation (3.9) is not the linear sum of equations (3.10) and (3.11). This would only be a good approximation for $\theta << 1$, as may be shown by expanding the exponentials in Taylor series and neglecting higher-order terms.

TRANSPORT THROUGH A POROUS DIAPHRAGM

To determine the applicability of the convective diffusion theory to porous systems, studies were next conducted with a porous diaphragm. Initially, it was not clear what role the porosity might play in the theory. It might be expected that redefinition of the Peclet number to include porosity would be necessary. Such redefinition would in all likelihood give rise to ambiguities in the new definitions of flow area, path length, and the effective diffusion coefficient. At best statistical characterization would be required, involving an element of arbitrariness at some point. It was decided to incorporate the effect of porosity into the diffusion coefficient, leaving A and ℓ as the cross-sectional area and membrane thickness, respectively. The nature of the experiment did not allow evaluation of this decision.

For steady state, net transport across the diaphragm is assumed given by equation (3.9) with the definitions discussed above. If solute moves into a compartment of volume V at position ℓ, then solute concentration in that volume will change with time. If the volume of the membrane is small, say less than 10 percent, compared to V, then to a good approximation $Q_N = V\, dC_\ell/dt$. Combination of this expression with equation (3.9) yields

$$V \frac{dC_\ell}{dt} = Q \frac{C_o e^\theta - C_\ell}{e^\theta - 1} \tag{3.12}$$

This equality is reasonable if C_ℓ changes slowly, as will be the case. Using the conditions $C_\ell(t=0) = C^\circ_\ell$ and $\lim_{t\to\infty} C_\ell = C^\infty_\ell$, integration of equation (3.12) leads to

$$\frac{C^\infty_\ell - C_\ell}{C^\infty_\ell - C^\circ_\ell} = e^{-\frac{t}{\tau}} \tag{3.13}$$

where $\tau = \frac{\ell V}{DA} \frac{e^\theta - 1}{\theta}$ is the convective diffusion time constant and $C^\infty_\ell = C_o e^\theta$. Since $\ell V/DA = \tau_D$ is the diffusion time constant, it follows that

$$\frac{\tau}{\tau_D} = \frac{e^\theta - 1}{\theta} \tag{3.14}$$

A sintered glass filter 20 mm diameter x 2 mm thickness, 5 μ nominal pore size, was chosen for the diaphragm. The solute was KCl. Description of the experimental system has been given by Overman (1968b). Only the results will be discussed here.

First, a transient diffusion experiment was performed as described by Robinson and Stokes (1959). Then, experiments were conducted with various

induced flow rates. Table 3.1 gives the results of these experiments, all conducted at 25°C. A time constant is not available for $\theta = -5.313$ due to irregularity in the bath during that run. It is apparent from column two that values obtained for DA/ℓ from the flow experiments agree quite well with that measured in the diffusion experiment. Also agreement between the calculated and observed time constant ratios is reasonably good. These results indicate that net transport of ions is adequately described for this system by equation (3.9).

As pointed out above, values for D, A and ℓ were not obtainable from this experiment; only the group DA/ℓ was evaluated. Such is the case because of the assumption that membrane volume was negligible compared to the volume of the end chamber, i.e., storage of ions within the membranes is negligible. Hence, no capacitance term appears in the transient solution.

TRANSPORT THROUGH A CLAY PLUG

A brief discussion of the applicability of convective diffusion theory to ion transport through compacted clay now follows, a more detailed discussion having been given by Overman (1968c). For this purpose, data was taken from the literature for two similar systems. Both studies used bentonite clay under steady state conditions. Since concentration distributions were measured, equation (3.4) is used for analysis. The Peclet number is defined as before, with the effect of the tortuous flow path being included in the system diffusion coefficient.

Table 3.1. Results for Porous Diaphragm Experiments.

θ	$\frac{DA}{\ell}$, $\frac{cm^3}{day}$	% Error	$\frac{\tau}{\tau_D}$ calc	$\frac{\tau}{\tau_D}$ obs	% Error
0	2.859	-	-	-	-
-1.383	2.914	+1.92	0.542	0.468	-15.8
-2.711	2.831	-0.98	0.344	0.366	+ 6.0
-5.313	2.861	+0.07	-	-	-
-7.440	2.914	+1.92	0.134	0.135	0.7

Figure 3.2 shows results for data taken from Kemper and van Schaik (1966). The corresponding distribution equation is

$$\frac{C - C_\ell}{C_o - C_\ell} = 1 - \frac{e^{-1.24x/\ell} - 1}{e^{-1.24} - 1} \qquad (3.15)$$

Agreement between data points and equation (3.15) is within 7 percent throughout the column. Further analysis showed that the ratio convective transport/diffusive transport was 0.47. However, the calculated solution flow rate is higher than measured. Also, the calculated diffusion coefficient $1.90 \cdot 10^{-5}$ cm^2/sec is too large.

Figure 3.3 applies to data taken from Dutt and Low (1962). In this case the distribution equation is

$$\frac{C - C_\ell}{C_o - C_\ell} = 1 - \frac{1 - e^{-0.80x}}{1 - e^{-0.80}} \qquad (3.16)$$

Agreement between data points and equation (3.16) is better than 3 percent. The calculated diffusion coefficient $6.54 \cdot 10^{-6}$ cm^2/sec is nearer to the expected value. Streaming rate was not measured. Relative transport was calculated as 17 percent for this experiment.

The ability of equation (3.4) to describe observed concentration distributions might be taken as evidence for the validity of convection diffusion theory. Application of different salt concentrations to two ends of a clay plug can induce osmotic transfer of water, as shown by Kemper and van Schaik (1966). This should lead to a nonlinear concentration profile. In addition, however, the theory should lead to a realistic estimate of the

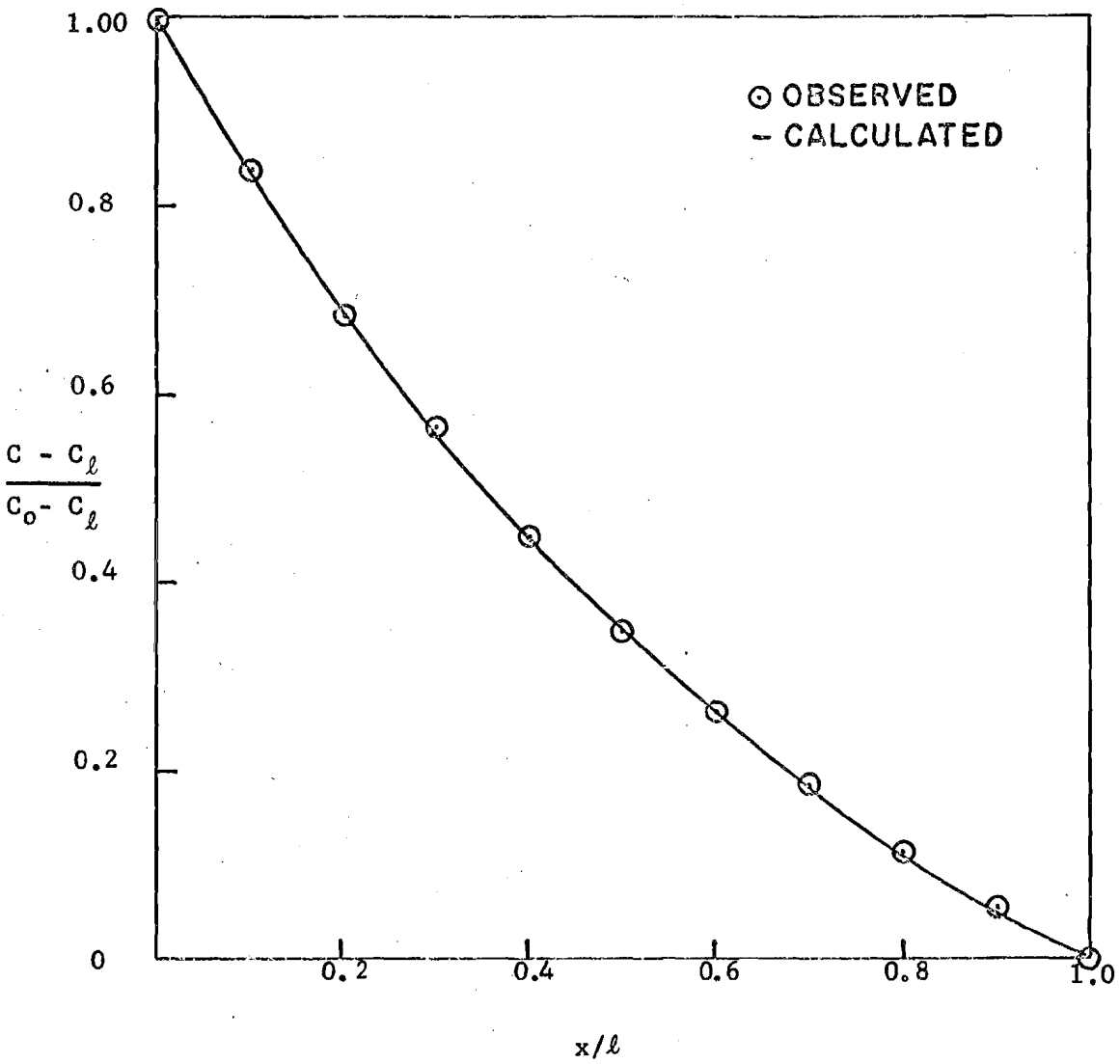

Figure 3.2. Analysis of experiment of Kemper and van Schaik (1966).

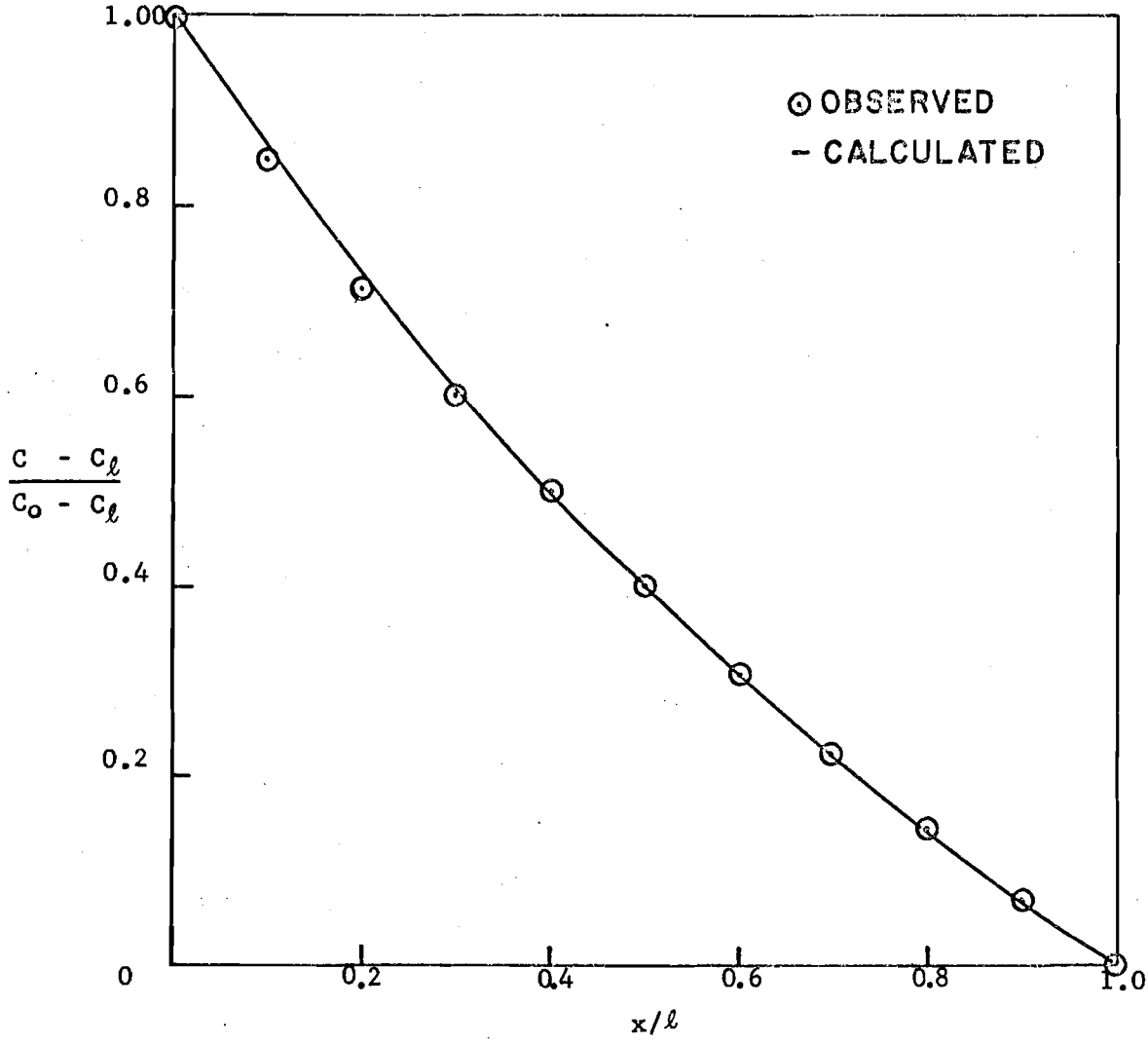

Figure 3.3. Analysis of experiment of Dutt and Low (1962).

diffusion coefficient. Analysis above showed failure to do so in at least one of the experiments.

It was suggested by Kemper and van Schaik (1966) that the curvilinear distribution was probably due to nonuniform distribution of clay in the plug. At the end with lower salt concentration, swelling pressure would be higher than at the opposite end, leading to migration of clay particles, eventually attaining a stable state. In turn, one would expect a variable diffusion coefficient D(x).

Following this suggestion the diffusion coefficient is assumed to have the form

$$D = D_o \, e^{kx/\ell} \tag{3.17}$$

where D_o is the diffusion coefficient at x = 0 and k governs the rate of change of the coefficient with position. Combining equations (3.8) and (3.15), and performing the integration, leads to

$$\frac{C - C_\ell}{C_o - C_\ell} = 1 - \frac{\exp\left(\theta_o \frac{1 - e^{-kx/\ell}}{k}\right) - 1}{\exp\left(\theta_o \frac{1 - e^{-k}}{k}\right) - 1} \tag{3.18}$$

where $\theta_o = \ell Q / D_o A$. For k = 0 (constant diffusion coefficient) equation (3.18) reduces to equation (3.4). For $\theta_o = 0$ (no streaming) the reduced form is

$$\frac{C - C_\ell}{C_o - C_\ell} = 1 - \frac{1 - e^{-kx/\ell}}{1 - e^{-k}} \tag{3.19}$$

which is the form of equation (3.4) for $\theta < 0$. Hence, the alternative explanation of the curvilinearity is also plausible.

It should be apparent from this discussion that quantitative description of ion transport through clays which exhibit swelling pressure becomes somewhat complex. This is not to dismiss the existence of convective diffusion in such systems, but indicates that quantification is elusive. Perhaps the treatment given here provides some insight as to proper approach.

TRANSPORT THROUGH A SAND COLUMN

Experiments similar to those for the porous diaphragm were conducted with sand. A sand column 1.00 cm thick and 3.75 cm diameter was mounted in a plastic tube between stainless steel screens. A solution of KCl was maintained at fixed concentration C_o at $x = 0$ by continuous recharge of approximately 1 liter per day. Concentration C_ℓ at $x = 1$ was measured with time by use of a conductivity cell and impedance bridge. Stirring of the solutions was accomplished with magnetic bars rotating at 30 rpm. The flow assembly was mounted in a thermostat at 30^oC, with control of $\pm 0.02^oC$.

A diffusion experiment was first performed to determine the diffusion coefficient. The column was mounted in a horizontal position to avoid natural convection due to density variations. Beneath the column 10^{-2} N KCl was maintained. Distilled water filled the column and upper chamber initially. The continuity equation, along with initial and boundary conditions, for the system are

$$0 < x < \ell \qquad \frac{\partial^2 C}{\partial x^2} - \frac{1}{D}\frac{\partial C}{\partial t} = 0$$

$$
\begin{aligned}
& & C(x,0) &= 0 \\
x = 0 & & C(0,t) &= C_o \\
x = \ell & & C(\ell,0) &= 0
\end{aligned}
\qquad (3.20)
$$

$$
\frac{\partial C}{\partial x} + \frac{1}{D\phi}\frac{\partial C}{\partial t} = 0
$$

where ϕ = volume of sand column/volume of upper chamber, being approximately unity for this experiment. The solution to boundary-value problem (3.20) is found by Laplace transform to be

$$
1 - \frac{C_\ell}{C_o} = 2 \sum_{n=1}^{\infty} \frac{\lambda_n^2 + \phi^2}{\lambda_n^2 + \phi^2 + \phi} \frac{\sin \lambda_n}{\lambda_n} e^{-\frac{D\lambda_n^2 t}{\ell^2}} \qquad (3.21)
$$

where λ_n are the roots of $\lambda_n \tan \lambda_n = 0$. Observed transient response is shown in Figure 3.4. After 24 hours the data are seen to form a straight line. Regression analysis of the data inclusive of 24 and 72 hours yields the equation

$$
1 - \frac{C_\ell}{C_o} = 1.1220 \; e^{-0.01544\, t} \qquad (3.22)
$$

with t in hours. In this time region only the leading term on the right side of equation (3.21) remains appreciable so that

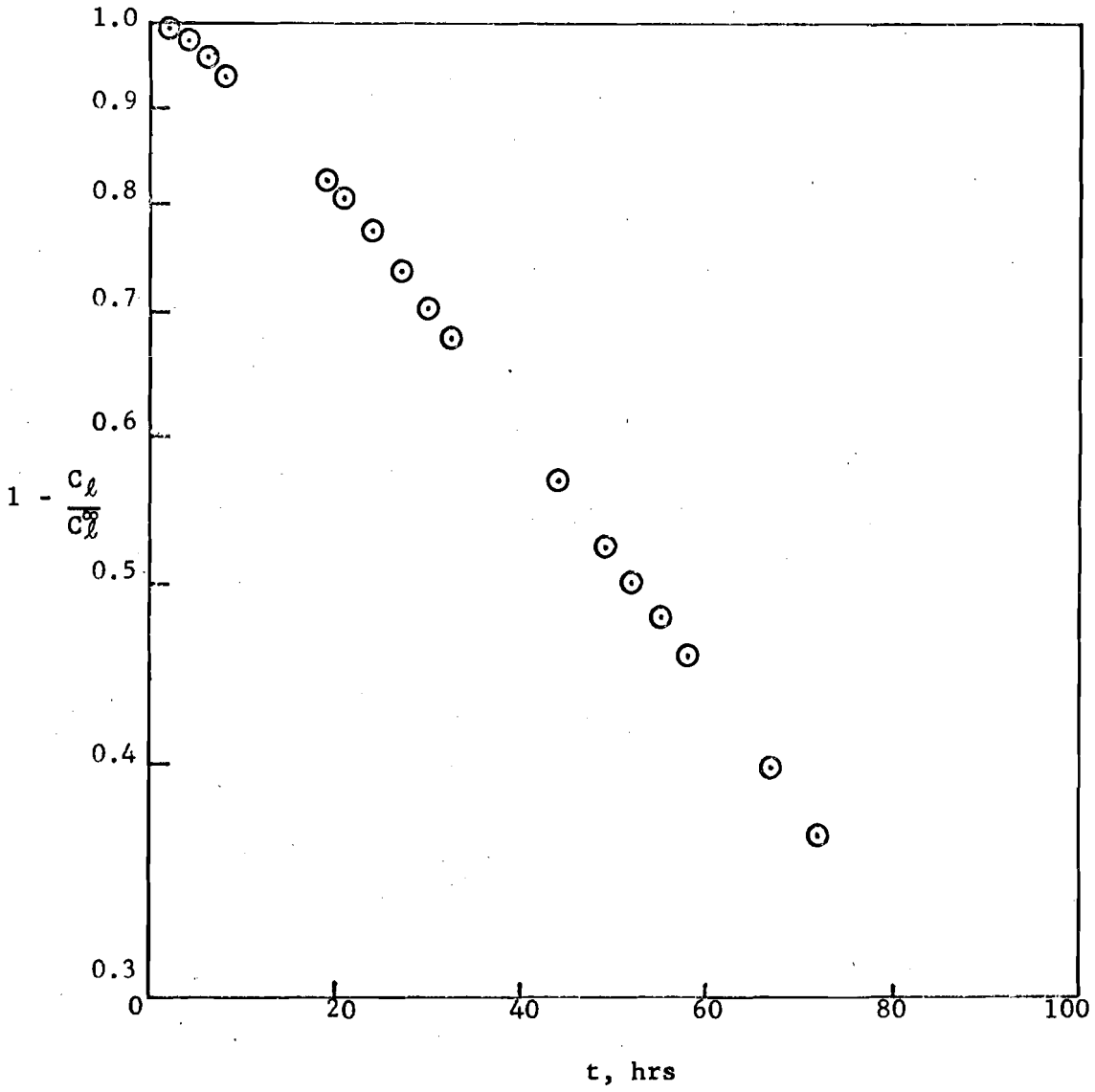

Figure 3.4. Transient diffusion experiment for sand column.

$$2\,\frac{\lambda_1^2 + \phi^2}{\lambda_1^2 + \phi^2 + \phi}\qquad \frac{\sin \lambda_1}{\lambda_1} = 1.1220 \tag{3.23}$$

$$\frac{D\lambda_1^2}{\ell^2} = 0.01544$$

hold. Carslaw and Jaegar (1959) give a table for the root equation from which we obtain $\phi = 1.04$ and $\lambda_1 = 0.8720$ to satisfy the first of equations (3.23). From the second equation it follows that $D = 5.64 \cdot 10^{-6}$ cm^2/sec, about one-fourth the solution value. In turn we calculate $DA/\ell = 5.380$ cm^3/day.

Following the diffusion experiment flow was induced into the upper chamber with a Harvard syringe pump and Hamilton leak-free syringe. In these experiments C_o was maintained at 1 N KCl. Results from Overman (1968d) are summarized in Table 3.2. It is concluded that equation (3.9) accurately predicts steady state transport through sand for Peclet numbers of magnitude below 10. Applicability of the theory beyond this range was not checked.

No difficulty seems to arise with definitions of the terms. It appears sufficient to include the effect of tortuosity in the system diffusion coefficient. This is convenient from an application standpoint. It would be useful, of course, to predict the diffusion coefficient from measurement of such factors as void ratio and particle size.

Table 3.2. Results for Sand Column

θ	DA/ℓ, cm^3/day	% Error	C^{∞}_{ℓ}/C_o
0	5.380	-	1.000
-5.519	5.369	-0.20	$4.010 \cdot 10^{-3}$
-7.725	5.370	-0.20	$4.416 \cdot 10^{-4}$

LITERATURE CITED

Bird, R. B., W. E. Stewart, and E. N. Lightfoot. 1960. Transport phenomena. John Wiley and Sons, Inc., New York.

Carslaw, H. S. and J. C. Jaeger. 1959. Conduction of heat in solids. 2nd edition. Oxford University Press, London.

Cole, G.H.A. 1962. Fluid dynamics. John Wiley and Sons, Inc., New York.

Darcy, H. 1856. Les Fontaines Publique de la Ville de Dijon. Victor Dalmont, Paris.

Derjaguin, B. V. and N. A. Krylov. 1944. Anomalies observed in the flow of liquids through hard fine-porous filters. "Proceedings of the Conference on Viscosity of Liquids", Vol. 2, pp. 52-53. U.S.S.R. Acad. Sci. Press, Moscow.

Dutt, G. R. and P. F. Low. 1962. Diffusion of alkali chloride in clay-water systems. Soil Sci. 93:233.

Hansbo, S. 1960. Consolidation of clay with special reference to influence of vertical drains. Swed. Geotech. Inst. Proc. 18, Stockholm.

Jackson, R. D. 1967. Osmotic effects on water flow through a ceramic filter. Soil Sci. Soc. Am. Proc. 31:713-715.

Kemper, W. D. 1960. Water and ion movement in thin films as influenced by the electrostatic charge and diffuse layer of cations associated with clay mineral surfaces. Soil Sci. Soc. Am. Proc. 24:10-16.

Kemper, W. D. and J. C. van Schaik. 1966. Diffusion of salts in clay-water systems. Soil Sci. Soc. Amer. Proc. 30:534.

King, F. H. 1898. Principles and conditions of the movement of ground water. U.S. Geol. Survey 19th Ann. Rept., part 2: 59-294.

Klute, A. 1965. Laboratory measurement of hydraulic conductivity of saturated soil. In Methods of soil analysis. Amer. Soc. Agron., Madison, Wisc.

Li, S. P. 1963. Measuring extremely low flow veolcity of water in clays. Soil Sco. 95:410-413.

Low, P. F. 1955. Effect of osmotic pressure on diffusion rate of water. Soil Sci. 80:95-100.

Low, P. F. 1961. Physical-chemistry of clay-water interaction. Advances in Agronomy. 13:269-327.

Lutz, J. F. and Kemper, W. D. 1959. Intrinsic permeability of clay as affected by clay-water interaction. Soil Sci. 88:83-90.

Martin J. F. 1962. Adsorbed water on clay: a review. Clays and Clay Minerals. 9:28-70. Pergamon Press, Inc., New York.

Micheals, A. S. and C. S. Lin. 1954. Permeability of kaolinite. Ind. Eng. Chem. 46:1239-1246.

Micheals, A. S. and C. S. Lin. 1955. Effects of counterelectro-osmosis and sodium ion exchange on permeability of kaolinite. Ind. Eng. Chem. 47:1249-1253.

Miller, R. J. and P. F. Low. 1963. Threshold gradient for water flow in clay systems. Soil Sci. Soc. Am. Proc. 27:605-609.

Mitchell, J. K. and J. S. Younger. 1967. Abnormalities in hydraulic flow through fine-grained soils. Permeability and Capillarity of Soils, A.S.T.M. STP 417, Amer. Soc. Testing Mats., p. 106.

Oakes, D. J. 1960. Solids concentration effects in bentonite drilling fluids. Clays and Clay Minerals 8:252-273. Pergamon Press, Inc., New York.

Olsen, H. W. 1965. Deviations from Darcy's Law in saturated clays. Soil Sci. Soc. Am. Proc. 29:135-140.

Olsen, H. W. 1966. Darcy's Law in saturated kaolinite. Water Resources Research 2:287-295.

Overman, A. R. 1965. Net molecular transfer in a capillary with diffusion and laminar flow. Unpublished Ph.D. Thesis.

Overman, A. R. and R. J. Miller. 1968. Convective diffusion in capillaries. J. Phys. Chem. 72:155.

Overman, A. R. 1968a. Transient convective diffusion in capillaries. J. Phys. Chem. (In press).

Overman, A. R. 1968b. Convective diffusion across a porous diaphragm. (Submitted for publication).

Overman, A. R. 1968c. Convective diffusion in clay systems. Soil Sci. Soc. Amer. Proc. (In press).

Overman, A. R. 1968d. Convective diffusion through a sand column. (Unpublished results).

Robinson, R. A. and R. H. Stokes. 1959. Electrolyte solutions. 2nd. edition. Academic Press, Inc., New York.

Taylor, G. I. 1953. Dispersion of soluble matter in solvent flowing slowly through a tube. Proc. Roy. Soc. A. 219:186.

von Engelhardt, W. and W. L. M. Tunn. 1954. The flow of fluids through sandstones (translated by P. A. Witherspoon from Heidelberger Beitrage Zur Mineralogie and Petrographie 2:12-25. 1954). Illinois State Geol. Survey Circ. 194.